RESEARCH PAPER

Acta Neurobiol Exp 2026, 86: 158–175
DOI: 10.55782/rv17ns77

Anatomy and retrograde connectivity of the septal nuclei in the Göttingen minipig

Asbjørn Lanng Thaysen[1,2], Johannes Bech Steinmüller[1], Carsten R. Bjarkam[3], Jens Christian H. Sørensen[1,2], Dariusz Orlowski[1,2]*

[1] *Center for Experimental Neuroscience, Department of Neurosurgery, Aarhus University Hospital, Aarhus, Denmark*
[2] *Department of Clinical Medicine, Aarhus University, Aarhus, Denmark*
[3] *Department of Neurosurgery, Aalborg University Hospital, Aalborg, Denmark*
* *Email: dorl@clin.au.dk*

The basal forebrain septum separates the lateral ventricles and comprises the *septum pellucidum* and *septum verum*, the latter containing the septal nuclei. These nuclei are involved in cognitive, emotional, and autonomic function and are implicated in psychiatric and neurological disorders, including Alzheimer's disease. However, their detailed organization and connectivity remain insufficiently characterized in translational large-animal models. In the present study, we investigated the anatomy and connectivity of the septal nuclei in the Göttingen minipig. Brain tissue was processed using Nissl staining and choline acetyltransferase immunohistochemistry, and neuronal connectivity was examined using magnetic resonance imaging-guided stereotaxic tracer injections. The septum comprises medial, lateral, posterior, and ventral complexes with distinct cytoarchitectonic features. Cholinergic neurons were primarily located within the medial septal complex. Both medial and lateral septal nuclei received widespread afferent projections from cortical, limbic, diencephalic, and brainstem regions, including the hippocampus, amygdala, hypothalamus, thalamus, ventral tegmental area, and periaqueductal grey. The medial septal nuclei showed relatively stronger inputs from prefrontal cortical regions, whereas the lateral septal nuclei received more prominent projections from brainstem structures. Reciprocal intrinsic connections within the septal region were also observed. These findings extend current knowledge of septal organization in the Göttingen minipig and support its use as a model for studying septal circuitry and related disorders.

Key words: Göttingen minipig; septum; septal nuclei; neuronal tracing; basal forebrain; connectivity; neuroanatomy

INTRODUCTION

The septum is a midline basal forebrain structure composed in humans of the *septum pellucidum* and the *septum verum*, which contains septal nuclei (SeN). The *septum pellucidum* is a thin membrane separating the lateral ventricles beneath the corpus callosum, whereas the SeN are located ventrally and comprise the medial, lateral, ventral, and posterior septal complexes (Andy & Stephan, 1961, 1968; Swanson & Cowan, 1979; Puska et al., 2024). As part of the limbic system, the SeN integrate limbic, hypothalamic, and brainstem information (Roxo et al., 2011; Kamali et al., 2023), and contribute to diverse physiological and behavioral functions, including neurodevelopment (Seminara et al., 2003; Pompolo et al., 2005), maternal behavior (Cruz & Beyer, 1972; Numan, 2000; Meza et al., 2015), and the reward-processing (Fisher, 2015).

The medial septal complex consists of the medial septal nuclei (MSN) and the vertical limb of the diagonal band of Broca (VLDB), together often referred to as the medial septum–diagonal band complex (MSDB). Along with the horizontal limb of the diagonal band (HLDB) and the nucleus basalis of Meynert (NBM), these nuclei form a major cholinergic component of the basal forebrain that provides the principal cho-

Received 18 June 2026, accepted 22 July 2026

linergic input to the hippocampus (Swanson & Cowan, 1979; Parent & O'Reilly-Fromentin, 1982; Mesulam et al., 1983; Mahady et al., 2017; Steinmuller et al., 2021; Takeuchi et al., 2021). Because these cholinergic projections are highly vulnerable to degradation in neurodegenerative conditions such as Alzheimer's disease, identifying them in a translationally relevant large-animal model is important for testing targeted clinical interventions (Takeuchi et al., 2021; He et al., 2023).

Notably, the structural classification of these septal areas is not uniform across mammalian reference frameworks. The Allen Mouse Brain Atlas segregates rodent lateral and medial septal complexes based on embryological development, grouping them under distinct ontogenetic categories: the striatum and pallidum, respectively (Oh et al., 2014). Human reference atlases, by contrast, favor a macroscopic, topographic approach, grouping these same regions under the broad umbrella of basal forebrain structures (Ding et al., 2016). This discrepancy does not reflect a known biological difference in wiring between species; rather, it stems from a historical preference for developmental tracking in small animals *versus* region-based topography in human brain mapping. Establishing a detailed baseline map of these structures in a large-animal model like the Göttingen minipig is therefore essential to help bridge these disparate species-specific nomenclature conventions.

Rodent studies further demonstrate dense afferent connectivity between the SeN and the hippocampus, prefrontal cortex, amygdala, hypothalamus, thalamus, VTA, PAG, and brainstem reticular formation (Risold & Swanson, 1997b; Swanson & Cowan, 1979; Montagnese et al., 2008). The close spatial relationship of the SeN with major fiber pathways, including the fornix and *stria terminalis*, further supports their integrative role within broader basal forebrain – limbic circuits (Patel, 2022; Kamali et al., 2023).

Despite the functional significance of the septal region, its anatomy and connectivity have not yet been systematically characterized in the porcine brain. The Göttingen minipig (GM) is increasingly used in translational neuroscience because of its gyrencephalic brain, human-like white-to-grey matter ratio, and suitability for clinical imaging and neurosurgical procedures (Danielsen et al., 2000; Bjarkam et al., 2008, 2017; Ettrup et al., 2010, 2012; Sørensen et al., 2011; Dolezalova et al., 2014; Glud et al., 2016, 2017, 2024; Meidahl et al., 2016; Orlowski et al., 2017, 2019; Christensen et al., 2018; Winterdahl et al., 2019; Bech et al., 2020; Melia-Sorolla et al., 2020; Steinmuller et al., 2021; Zaer et al., 2022; Poulsen et al., 2026). Compared with small-animal models, the GM offers greater translational relevance while avoiding several of the ethical and logistical limitations associated with nonhuman primate research (Lind et al., 2007; Sørensen et al., 2011).

The present study provides an anatomical characterization of the septal region in the GM and describes the afferent connectivity of the medial and lateral septal nuclei using retrograde neuronal tract tracing. Although the HLDB and NBM are not traditionally classified as part of the SeN, they were included in this investigation due to their close anatomical and functional relationship with the medial septal complex (Mesulam et al., 1983; Mahady et al., 2017).

METHODS

Surgery

Six female GM (*Sus scrofa*, Göttingen Minipigs breed, Ellegaard Göttingen Minipigs APS, Dalmose, Denmark) aged 6-8 months, weighing 23.8-25.6 kg, were used in the tracing experiment. All procedures were approved by the Danish Animal Experiments Inspectorate (protocol number: 2018-15-0201-01435) and complied with ARRIVE guidelines and EU directive 2010/63/EU for animal experiments. Animals were premedicated intramuscularly with a mixture of 4 mL S-ketamine (20 mg/kg) and 6 mL midazolam (0.8 mg/kg), intubated, and maintained under sevoflurane anesthesia (2-3%; Abbott, USA) during mechanical ventilation (Jülian Dräger, Germany), as described previously (Ettrup et al., 2011). The head was fixed in a stereotaxic frame (Mark 2.5, Neurologic, Denmark) in the prone position. Screws were inserted bilaterally into the zygomatic bones after subcutaneous administration of bupivacaine (5 mg/ml) (Fig. 1a) (Bjarkam et al., 2004). Because the SeN are located in the midline, the head was tilted approximately 15° sideways away from the injection side to avoid damage to the superior sagittal sinus from the craniotomy (Fig. 1c). A fiducial marker was placed in a drill hole (Fig. 1b) (Glud et al., 2017), and the MRI was performed using a 3T Siemens Magnetom Prisma Fit scanner (Siemens, Germany), with T1-weighted 3D TurboFlash sequence as follows: voxel 1×1×1, slice 176, FOV 256×256 pixels, TR: 2420ms, TE: 3.7 ms, TI: 960 ms, Flip: 9°, Averages: 2. Images were reconstructed into isometric 1 mm^3 voxels (Bjarkam et al., 2004; Glud et al., 2017).

The retrograde FluoroGold tracer (FG Lot: BCBW6126, FluoroChrome, LLC, USA) and the anterograde tracer biotinylated dextran amine (BDA-10.000, NeuroTrace™ Neuronal Tracer Kit, Thermo Fischer,

USA) were dissolved in distilled water at concentrations of 4% and 20%, respectively, and mixed 1:1 to obtain a final concentration of 2% FG and 10% BDA (Sorensen et al., 1996; Poulsen et al., 2026). However, anterograde tracing was unsuccessful and, therefore, not included in the present study.

Septal coordinates were calculated relative to the fiducial (Fig. 1c, d). A TSE parallel rail stereotaxic and micromanipulator system (TSE System GmbH, Bad Hamburg, Germany) was attached to the head frame. A craniotomy was performed using a neurosurgical drill (Midas Rex, Medtronic, USA), the dura was opened, and the cortex exposed. Tracers were injected using a 5 µL Hamilton syringe (Hamilton, USA), mounted on the micromanipulator (Sorensen et al., 1996; Poulsen et al., 2026). After insertion into the target, the cannula was left in place for 2 min to allow tissue stabilization (Fig. 1e). Subsequently, 1 µL of tracer solution was injected at a rate of 0.1 µL/min over 10 min. After injection, the cannula remained in place for 5 min to allow tracer diffusion and minimize reflux, then was slowly retracted by 3 mm, held for an additional 2 min, and finally withdrawn completely. Three animals received injections into the LSN complex, and three into the MSN complex. Following injection, the craniotomy was filled with autologous bone paste, and the skin was closed with interrupted sutures (Fig. 1f). Animals were monitored daily postoperatively for changes in feeding, social interaction, locomotion, or signs of discomfort.

After a 4-week survival period, animals were deeply sedated and euthanized with an intracardiac overdose of pentobarbital (400 mg/mL, Exagon Vet, Richter Pharma, Austria). Then they were perfused with 5L of 10% buffered formalin (Ettrup et al., 2011). Brains were removed (Bjarkam, Orlowski, et al., 2017) and post-fixed in the same fixative for at least five days.

Histology

Fixed brains were embedded in histOmer alginate (Sorensen et al., 2000; Bjarkam et al., 2001), sectioned using a histOslicer (HistOtech, Aarhus, Denmark) into 2 cm slabs, and cryoprotected in 30% sucrose (VWR) in Sørensen's phosphate buffer (PB), for 8-12 days (Bjarkam, Glud, et al., 2017; Bjarkam et al., 2001), until the tissue sank. Then, tissue slabs were frozen in isopentane (2-methylbutane, Sigma), cooled to approximately -50˚C with dry ice, and sectioned coronally on a cryostat (CryoStar NX70, Thermo Scientific). Four series of every 20th 40 µm thick sections were collected. Two series were mounted on gelatin-coated slides, and the remaining two were stored in deOlmos cryoprotectant solution (30% sucrose, 30% ethylene glycol, 1% polyvinylpyrrolidone in PB), giving an in-

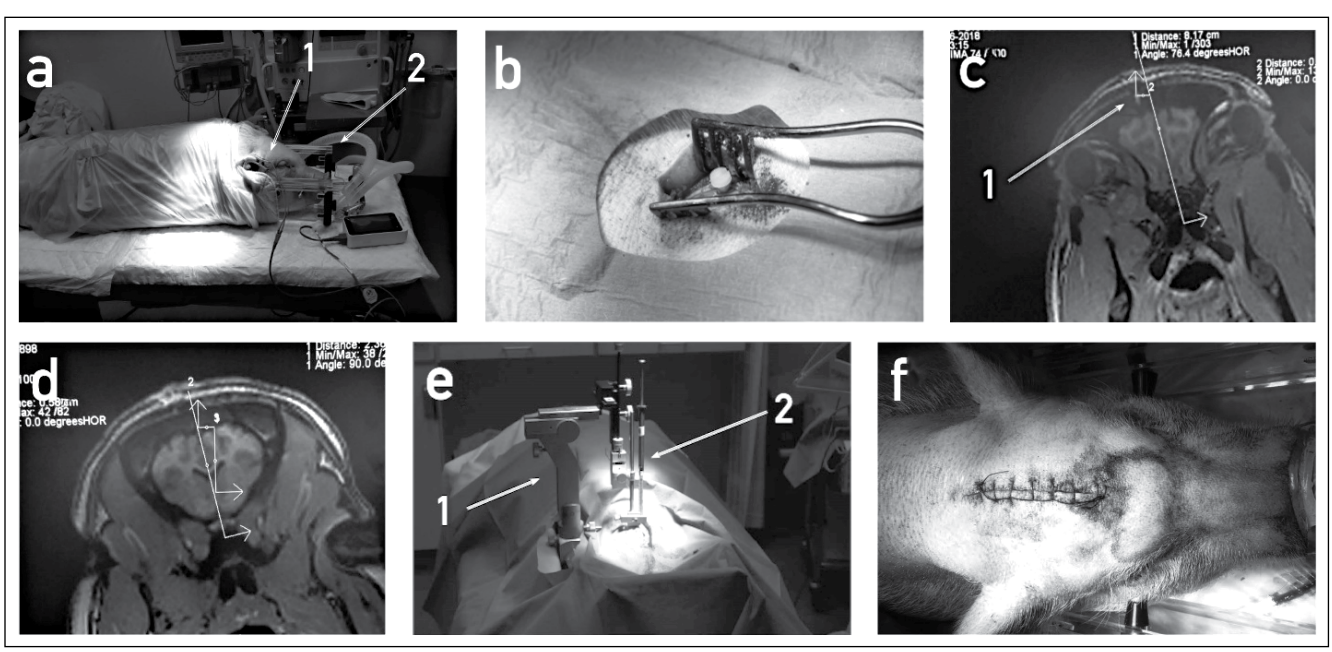

Fig. 1. MRI-guided stereotaxic tracer injection procedure in the Göttingen minipig. (a) The animal is positioned prone with the head secured in the stereotaxic frame (2) and a pulse-oximeter attached to the ear (1). (b) An MRI-compatible fiducial marker is placed in the burr hole. (c, d) Coordinates of the septal nuclei are calculated relative to the fiducial marker (1); the head is tilted approximately 15 degrees to avoid the superior sagittal sinus during injection. (e) A micromanipulator (1) mounted on the frame guides the Hamilton syringe containing tracer (2) into the brain. (f) Following injection, the syringe is withdrawn, and the wound is sutured.

terval of 800 µm distance between adjacent sections within each series.

For anatomical delineation of the septal nuclei, seven additional Göttingen minipig brains were processed identically. Six series of every 20th 40 µm thick sections were collected, including two mounted on gelatin-coated slides and four in deOlmos cryoprotectant.

Nissl staining was performed using 0.1% toluidine blue in 0.1 M citrate buffer for 9 min. Sections were differentiated in 99.9% ethanol, cleared in xylene, and coverslipped with Depex.

For choline acetyltransferase (ChAT) immunostaining, free-floating sections were rinsed in Tris-buffered saline (TBS) containing 1% Triton X-100 (TBS-T, pH 7.4). Endogenous peroxidase activity was quenched in 3% H_2O_2 in TBS for 10 min. Sections were preincubated for 30 min in 1% normal horse serum (NHS, lot: GR3217249-1, Abcam) in TBS and incubated overnight at 4°C with goat anti-ChAT primary antibody (1:1000, AB144P, lot: 2908690, Millipore). Then, sections were incubated with biotinylated horse anti-goat IgG (1:200) for 1 hour, followed by ABC complex solution (Vector Laboratories) for 1 hour. Immunoreactivity was visualized with 0.1% DAB and H_2O_2. Sections were mounted on gelatin-coated slides, air-dried, and coverslipped with Depex.

Tracer visualization

For FG visualization, the sections were dehydrated with xylene and coverslipped using Depex. FG-positive neurons were interpreted as retrogradely labelled cells. Neuroanatomical identification of nuclei was based on published porcine atlases and anatomical studies (Felix et al., 1999; Larsen et al., 2004; Ettrup et al., 2010; Meidahl et al., 2016; Mahady et al., 2017; Bjarkam, Glud, et al., 2017, 2024; Orlowski et al., 2019; Bech et al., 2020), together with the online minipig brain atlas available at cense.au.dk. Projection strength was semi-quantitatively assessed according to the number of FG-positive neurons per target area: + (<24 cells), ++ (25-49 cells), +++ (50-199 cells), ++++ (>200 cells) (Table 1).

Imaging

Sections were examined using a Leica DM5000B microscope equipped with a Leica DMC480 digital camera. Images were processed and assembled using Adobe Photoshop and Illustrator CC 2019 (Adobe Inc.), and GIMP (3.2.4).

RESULTS

Septum anatomy

The septum of the Göttingen minipig consists of the *septum verum* with the septal nuclei and a thin, non-neuronal *septum pellucidum*. The *septum pellucidum* is a tissue membrane separating the lateral ventricles and appearing as a continuation of the dorsal lateral septal nuclei, fimbria, and hippocampus. The SeN are located in the midline part of the medial forebrain, ventral to the corpus callosum and the *septum pellucidum*. Approximate dimensions measured *via* MRI were: anteroposterior 6 mm, dorsoventral 10 mm, and lateral 4.5 mm. Rostrally, the SeN are bordered by the *indusium griseum* (IG), Brodmann areas 25 and 33 homologues (BA25 and BA33, respectively), the *tenia tecta* (tt), and the olfactory tubercle (Tu). Caudally, they are delimited by the diencephalon. The *septum pellucidum* and lateral ventricles define the dorsal border, while ventrally, the SeN are adjacent to the anterior olfactory nucleus, nucleus accumbens, and the preoptic part of the hypothalamus. Laterally, they are bordered by the lateral ventricles, nucleus accumbens, and internal capsule (Fig. 2). In the GM, the SeN can be subdivided into medial, lateral, posterior, and ventral septal complexes. Bilateral septal complexes are symmetrical in position, shape, and cellular morphology.

Medial septal complex

The medial septal complex consists of the medial septal nucleus (MSN) and the vertical limb of the diagonal band of Broca (VLDB). In the coronal plane, the MSN is elongated; in the horizontal plane, it assumes a J-shaped form, deviating laterally. Dorsally and laterally, the MSN is bordered primarily by the lateral septal complex (Fig. 2c-f). Ventrally, the MSN continues into the VLDB, which borders the hypothalamus and LSN before extending laterally as the horizontal limb of the diagonal band (HLDB, Fig. 2f-h).

Morphologically, the VLDB and MSN both contain large, darkly Nissl-stained neurons. Anti-ChAT staining distinguishes these regions as containing strongly labeled bipolar or multipolar cholinergic neurons. MSN cholinergic neurons are generally larger than those in the VLDB. Medially, a dense cluster of cells follows the medial border of MSN; laterally, neurons are more dispersed. VLDB's cholinergic neurons are positioned along the cerebral longitudinal fissure (Fig. 3).

Table 1. FluoroGold tracing results. Anatomical regions containing FG-positive cell bodies are sorted alphabetically. Retrograde projections are tracked into either the LSN (PIG01, PIG02, and PIG04) or the MSN (PIG05 and PIG06). The density of retrograde labeling is semi-quantified based on regional cell counts: (+), less than 24 cells; (++), 25 to 49 cells; (+++), 50 to 199 cells; (++++) greater than 200 cells. Abbreviations: Ipsi, ipsilateral; contra, contralateral. Projections within structures where hemispheres could not be reliably segregated, or where precise laterality remains uncertain, are classified as midline; these are marked with a hash sign (#) and indicated by a (+) sign centered between the ipsilateral and contralateral columns. *Labeled profiles identified within white matter pathways should be interpreted as passing fibers rather than the target structure.

	PIG01		PIG02		PIG04		PIG05		PIG06	
Location of injection	Dorsal/ intermediate LSN		Intermediate LSN		Intermediate/ ventral LSN		Bilateral MSN		Unilateral MSN	
Connection source	ipsi	contra	ipsi	contra	ipsi	contra	ipsi	contra	ipsi	contra
Amygdala	++++						+++	+++	++	+
Amygdalohippocampal area								+		
Amygdalopiriform area	++		+++				++	++	+++	
Anterior olfactory nucleus	++++						++++	+++	+++	+
BA25	+++	++					++++	++++	++++	+
BA33							+++	+++	++++	+
BNST	+		++		+		+	+	++	
*Cingulum**									++++	
Cortex	++++						+++	++	++	
DSCP*#	++++		++		+++		+++		+++	
Entorhinal cortex	+						+		+	
FLM*#	+++						++		+	
Habenula							+	+	+	
Hippocampus	++++	++++			++++	+++	++++	++++	++++	+++
HLDB	+++				+		+++		++++	+
Hypothalamus	++++		++++	+++	++++	+++	++++	++++	++++	+
IG	++++	++			+		+++	+	++++	+
Lateral lemniscus*#	++++									
LSN	++++		++++		++++		+++	+++	+++	
Mammillary body	++				+	+				
MSN	+++				++		++++	++++	++++	
NBM	++		+				+++		+++	+
IPN#	++++		++		+++		+++		++++	
Olfactory Tubercle					+		++	+		
PAG#	++++		++		+++		+++		+++	
Piriform cortex	++++						++	++		
Pontine nuclei#							+		+	
Prefrontal cortex	+++	+					+++	++		
RF#	+++				+		++			
RN	+++				+					
SCN	+++									
SF	+++		+++		++++		++++		++++	
Subfascicular nucleus							+	+		
Subfornical organ					+		+			
Substantia nigra	+++		+		+					
Supramammillary commissure*	++									
Tenia tecta	+++	+					+++	+++		
Thalamus	+++		+++		++		+++	+++	+++	+
Vestibular nucleus							+			
VLDB	++		+		+		+++		+++	+
VTA	++++	+++			++++	++	++++		++++	++
Zona incerta	++									

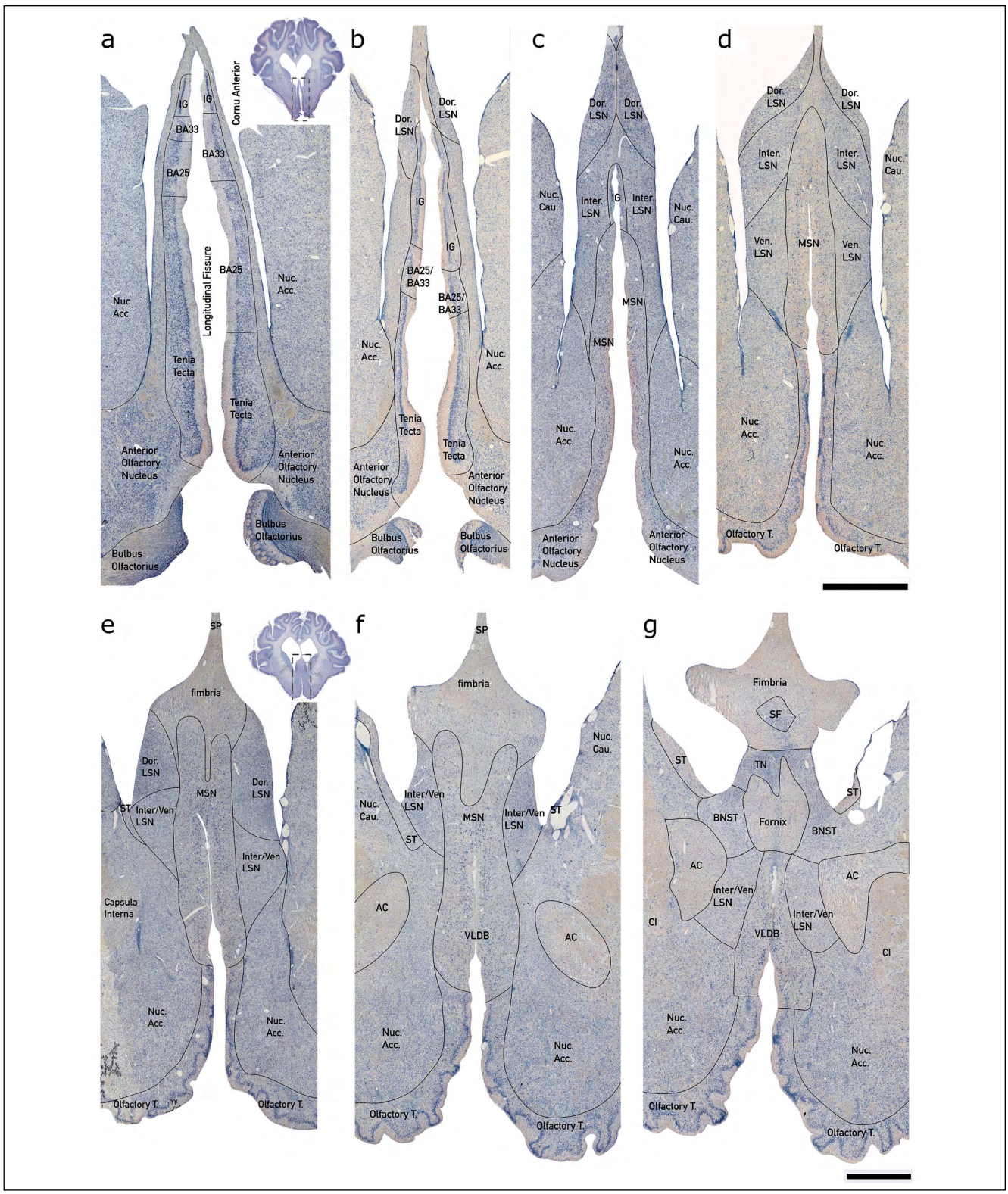

Fig. 2. Cytoarchitecture of the septal region in the Göttingen minipig. Consecutive coronal Nissl-stained sections arranged from rostral to caudal. (a-d) Anterior level of the septum. (e-g) Intermediate levels. (h, i) Caudal septal regions. (j, k) Posterior septal regions and adjacent structures. An insert at the top of the panels (a), (e), (h), and (j) shows the full coronal section with the magnified region indicated. Abbreviations: AC, anterior commissure; BA25, Brodmann area 25 homologue; BA33, Brodmann area 33 homologue; BNST, bed nucleus of the stria terminalis; CI, internal capsule; Dor. LSN, dorsal lateral septal nucleus; F, fornix; H, habenula; HLDB, horizontal limb of the diagonal band of Broca; IG, indusium griseum;

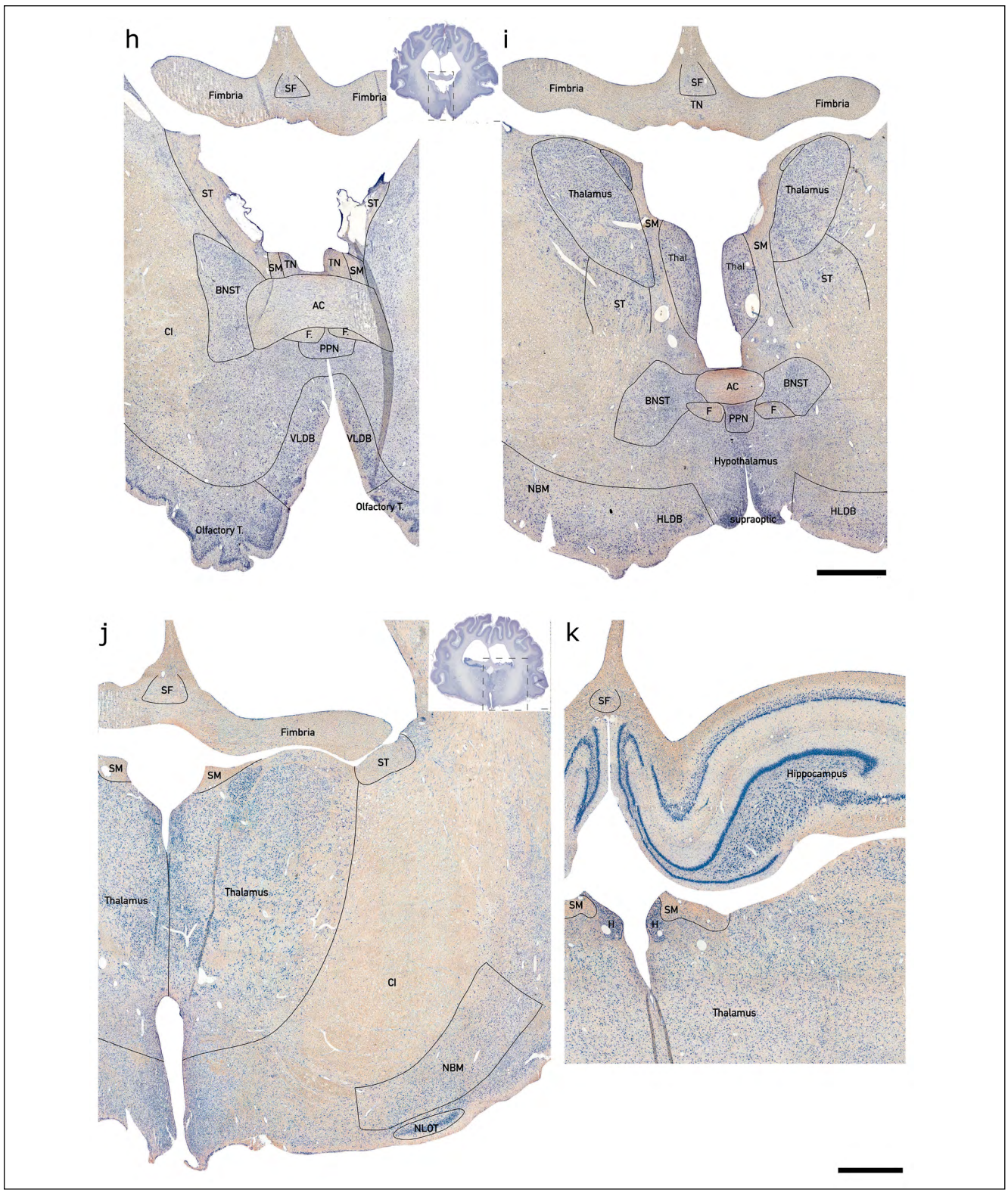

Inter. LSN, intermediate lateral septal nucleus; MSN, medial septal nucleus; NBM, nucleus basalis of Meynert; NLOT, nucleus of the lateral olfactory tract; Nuc. Acc., nucleus accumbens; Nuc. Cau., caudate nucleus; Olfactory T., olfactory tubercle; PPN, paramedian preoptic nucleus; SF, septofimbrial nucleus; SM, stria medullaris; SP, septum pellucidum; ST, stria terminalis; Thal, Thalamus; TN, triangular nucleus; Ven. LSN, ventral lateral septal nucleus; VLDB, vertical limb of the diagonal band of Broca. Scale bar=2 mm.

Lateral septal complex

The lateral septal complex comprises the lateral septal nucleus (LSN) and the septofimbrial nucleus (SF). The LSN is subdivided into dorsal, intermediate, and ventral groups. It extends from the IG, BA25/33 rostrally, to the anterior commissure and bed nucleus of the stria terminalis (BNST) caudally, and is bordered medially by the MSN. Caudally, the LSN turns ventral to the fimbria (Fig. 2b-g).

The dorsal subdivision contains darkly stained cells. The ventral and intermediate groups are histologically heterogeneous; however, neurons of the intermediate group appear larger on average than in the ventral group. The LSN contains no cholinergic neurons, though fiber-rich, AChT-positive areas were observed. The SF is situated within the fimbria (Fig. 2g-k), and is composed of lightly stained, medium-sized neurons arranged in compact clusters. Neither cholinergic neurons nor fibers were detected in this region.

Posterior and ventral septal complex

The posterior septal complex consists of the thin, horizontally elongated, triangular nucleus (TN) composed of densely packed, small, dark Nissl-stained neurons, and extending from the MSN and BNST along the ventral hippocampal commissure and fornix (Fig. 2g, k). Only very few cholinergic neurons were observed in this region. The ventral septal complex is represented by the BNST, adjacent to the stria terminalis and the anterior commissure (Fig. 2g-i). BNST cells are lightly Nissl-stained, medium-sized, and scattered, with a small number of ChAT-positive neurons and fibers detected.

The horizontal limb of the diagonal band of Broca and the nucleus basalis of Meynert

The VLDB extends laterally into the HLDB. Rostrally to the HLDB lies the olfactory tubercle, while caudally it is bordered by the hypothalamus. Dorsally, it is delimited by the internal capsule. Laterally, the HLDB continues into the NBM (Fig. 2i), which extends caudally to the level of the cerebral peduncle. Dorsally, the NBM borders the internal capsule and the globus pallidus, while laterally it is flanked by the globus pallidus and the prepiriform area (Fig. 2i, j).

The cholinergic MSN continues ventrally into the VLDB, which in turn extends laterally into the HLDB and further into the NBM. All four regions (MSN, VLDB, HLDB, and NBM) are predominantly cholinergic.

The HLDB and NBM are separated by the internal capsule (Fig. 2i). Both consist of large, darkly Nissl-stained neurons, similarly to those observed in MSN and VLDB. Neuronal dispersion increases laterally, with cells in the lateral part of the NBM appearing more widely spaced compared to those in the medial part of the HLDB. ChAT staining confirmed that the large neurons in both HLDB and NBM are cholinergic, as in the MSN and VLDB (Fig. 3). HLDB neurons were predominantly bipolar, whereas NBM neurons were multipolar or bipolar.

Septal connections

All six animals survived surgery without neurological deficits or other complications. Histological analysis confirmed correct targeting in five animals; one injection was misplaced in the lateral ventricle and excluded from connectivity analysis. Three animals received injections into the LSN, and two into the MSN (Fig. 4).

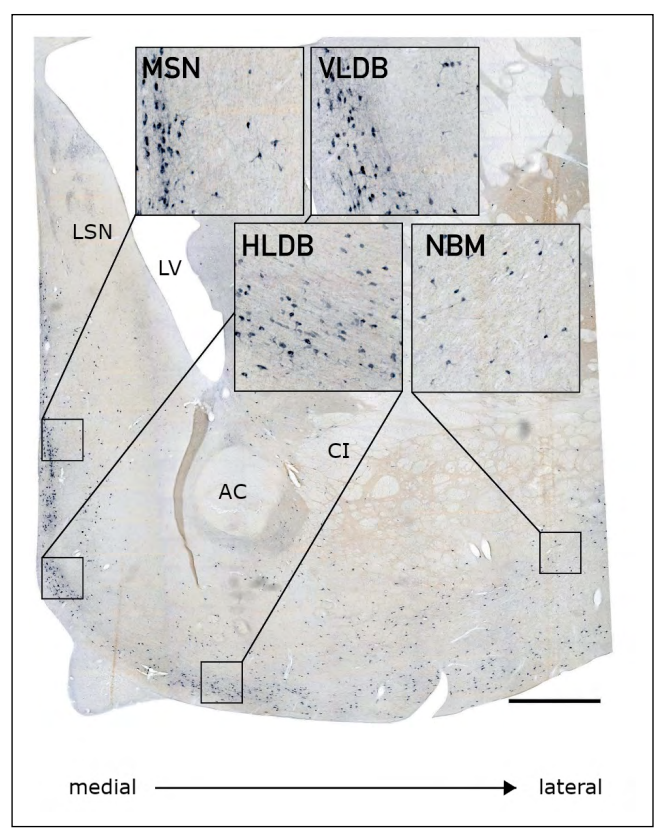

Fig. 3. Cholinergic organization of the septal region. Anti-ChAT immunostaining demonstrating cholinergic neurons in the medial septal nucleus (MSN), vertical limb of the diagonal band of Broca (VLDB), horizontal limb of the diagonal band of Broca (HLDB), and nucleus basalis of Meynert (NBM). The MSN displays a characteristic bilaminar organization, with densely packed medial neurons and more dispersed lateral cells. No ChAT-positive neuronal somata are observed in the lateral septal nucleus (LSN), although dense cholinergic fibers are present. Abbreviations: AC, anterior commissure; CI, internal capsule; LV, lateral ventricle. Scale bar = 2 mm.

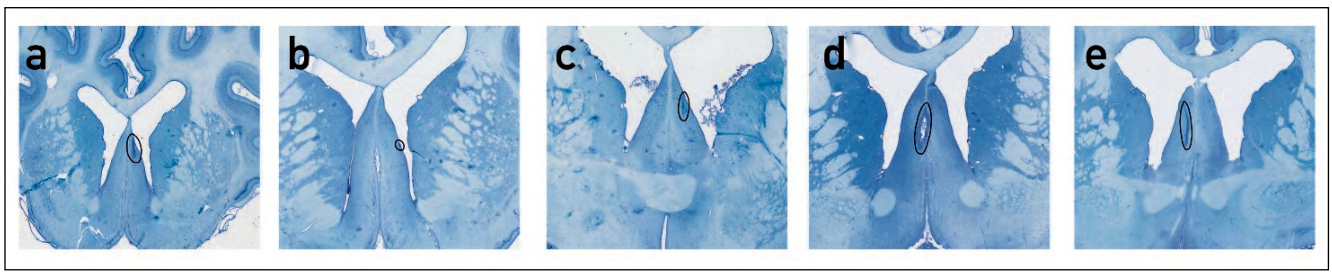

Fig. 4. Injection sites of neuronal tracers. Representative coronal Nissl-stained sections showing tracer injection sites indicated by black circles. (a) PIG01, dorsal/intermediate LSN; (b) PIG02, intermediate LSN; (c) PIG04, intermediate/ventral LSN; (d) PIG05, bilateral MSN; (e) PIG06, unilateral MSN.

Analysis of anterograde labeling with BDA was not feasible due to limited transport beyond the injection sites. Retrograde labeling with FG is summarized in Table 1. The projections were semi-quantified and categorized as ipsilateral or contralateral. However, in the brainstem, FG-positive cells were primarily located along the midline and were therefore interpreted as bilateral.

Numerous intrinsic septal connections were identified, as evidenced by FG-positive neurons within the septal complex. In addition, both LSN and MSN received afferent projections from the amygdala (except the pig 2 and 4), thalamus, hypothalamus, hippocampus, VTA, and PAG. The LSN received relatively stronger inputs from the brainstem structures, particularly the RF and the RN, whereas the MSN showed more prominent afferents from the prefrontal cortex.

Most projections were lateralized, with a predominance of ipsilateral labelling. FG-positive neurons were observed both rostral and caudal to the septum. Rostral projections originated mainly in the prefrontal cortex, passing through BA25 and the tenia tecta. Caudal projections followed two principal pathways: a dorsal route *via* the SF from the hippocampus, and a ventral route *via* the MSN, VLDB, hypothalamus, and VTA from the brainstem. Within the thalamus, labelling was most prominent in the anteromedial and centromedial nuclei. In the hypothalamus, FG-positive neurons were concentrated in the medial and lateral preoptic area and in the anterior, posterior, and lateral hypothalamic regions. Representative micrographs of FG-positive neurons are shown in Fig. 5.

FG tracer was also detected in the tissue bordering the lateral ventricles, indicating variable tracer leakage. This was most pronounced in the PIG02 and PIG03.

Retrograde tracing from the LSN

In PIG01 (injection to dorsal/intermediate LSN), numerous FG-positive neurons projecting to the LSN were identified in the prefrontal cortex, anterior olfactory nucleus, *indusium griseum* (IG), BA25, and the *tenia tecta*. Contralateral labeling was also present in these regions, but it was less prominent. Dorsocaudal labeling was observed within the ipsilateral LSN and SF, as well as bilaterally in the hippocampus. FG-positive neurons were found in the ipsilateral MSN, HLDB, amygdala, piriform cortex, thalamus, hypothalamus, *substantia nigra*, and bilaterally in the VTA, PAG, DSCP, IPN, RF, medial longitudinal fasciculus (FLM), lateral lemniscus, superior central nucleus (SCN), and RN. Additional ipsilateral projections arose from the VLDB, NBM, BNST, amygdalopiriform area, entorhinal cortex, mamillary body, supramammillary commissure, and *zona incerta*. FG-positive neurons were also observed along the injection tract in the cortical regions.

In PIG02 (injection to intermediate LSN), no rostral projections were detected. Dorsocaudally, FG-positive neurons were found in the ipsilateral LSN and SF. Ventrocaudal projections originated mainly from the ipsilateral amygdalopiriform area and the thalamus, and bilaterally from the hypothalamus. Additional inputs were observed from the ipsilateral HLDB, NBM, BNST, *substantia nigra*, and bilaterally from the PAG, DSCP, and IPN.

In PIG04 (injection ventral/intermediate LSN), projections originated from the olfactory tubercle and IG. Strong ipsilateral labeling was observed in the LSN and SF, with additional bilateral projections from the hippocampus. Sparse inputs arose from the subfornical organ. Ventrocaudal afferents included the ipsilateral VTA, and bilateral hypothalamus, PAG, DSCP, and IPN. Further projections were identified from the ipsilateral MSN, VLDB, HLDB, BNST, thalamus, *substantia nigra*, as well as from the contralateral VTA. Bilateral inputs were also present from the mamillary body, RF, and RN.

Retrograde tracing from the MSN

In PIG05 (injection to midline MSN), rostral projections from the prefrontal cortex, IG, anterior olfactory nucleus, BA25, BA33, *tenia tecta*, and the olfactory tubercle were observed. Additional inputs arose from the

LSN, SF, hippocampus, and, to a lesser extent, from the subfornical organ. Ventrocaudal projections originated from the MSN, VLDB, HLDB, NBM, amygdala, thalamus, hypothalamus, VTA, PAG, DSCP, and IPN. Further afferents were identified from the BNST, amygdalopiriform area, piriform cortex, entorhinal cortex, habenula, subfascicular nucleus, RF, FLM, and the vestibular nucleus.

In PIG06 (injection to unilateral MSN), we noted ipsilateral projections from the IG, anterior olfactory

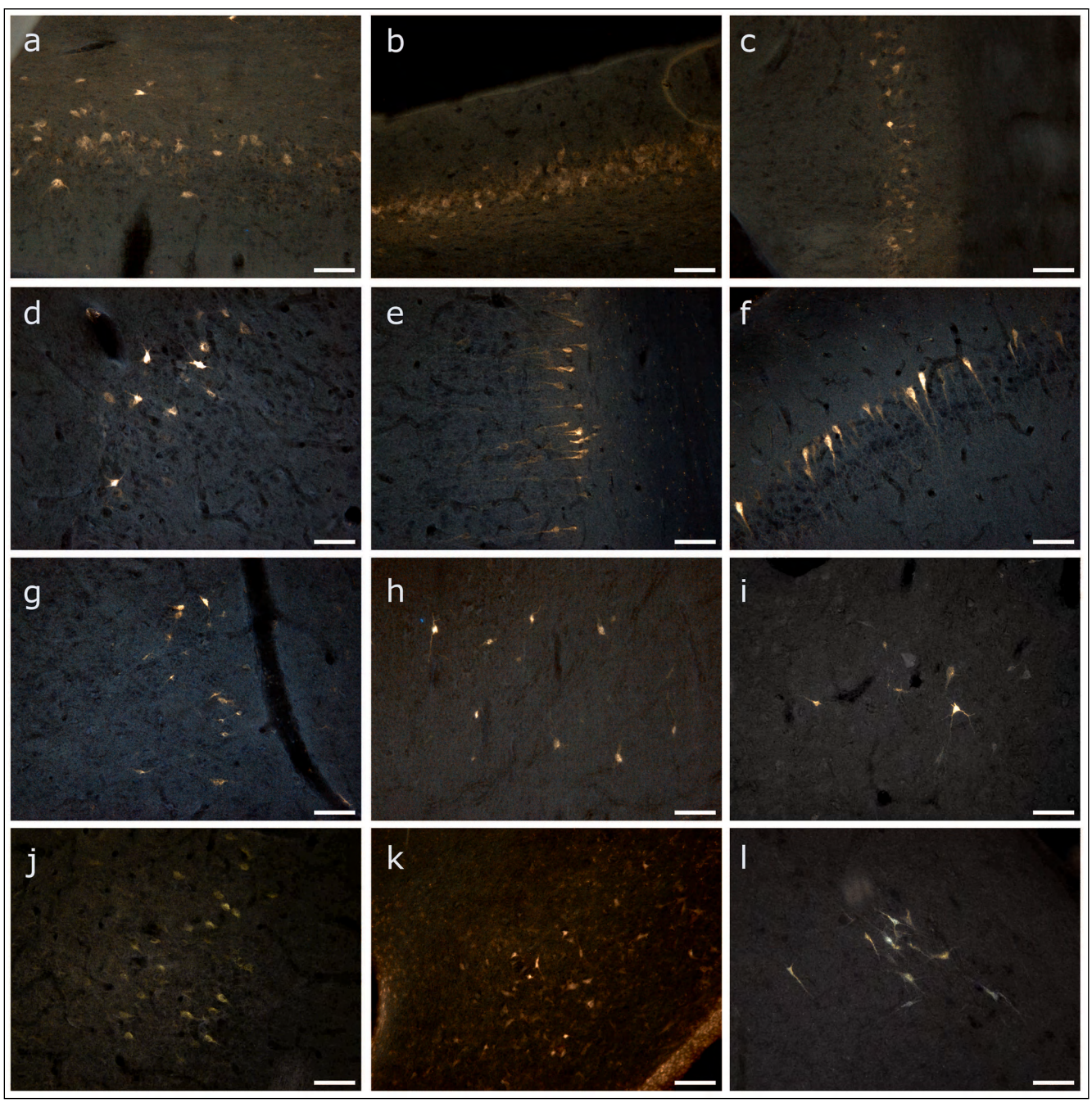

Fig. 5. Representative micrographs of retrogradely labeled, FG-positive neurons in major afferent regions. (a) PIG05, BA25, contralateral side; (b) PIG05, BA25, ipsilateral side; (c) PIG05, IG, contralateral side; (d) PIG05, amygdala, ipsilateral side; (e) PIG05, hippocampus, ipsilateral side; (f) PIG05, hippocampus, contralateral side; (g) PIG05, hypothalamus, ipsilateral side; (h) PIG05, VTA; (i) PIG05, PAG; (j) PIG01, prefrontal cortex, ipsilateral side; (k) PIG02, thalamus, ipsilateral side; (l) PIG02, hypothalamus, ipsilateral side. Abbreviations: BA25, Brodmann area 25 homologue; IG, indusium griseum; PAG, periaqueductal gray; VTA, ventral tegmental area. PIG01, FG injection to dorsal/intermediate LSN; PIG02, FG injection to intermediate LSN; PIG05, FG injection to bilateral MSN; Scale bar=100 μm.

nucleus, BA25, BA33, and, to a lesser extent, from the cortex, with weaker contralateral labeling in the same regions. Dorsocaudally, strong projections originated from the ipsilateral LSN and SF, and bilaterally from the hippocampus. Ventrocaudal inputs were dense from the ipsilateral MSN, VLDB, HLDB, NBM, amygdalopiriform area, thalamus, hypothalamus, and VTA, as well as bilaterally from the PAG, DSCP, and IPN. Additional FG-positive neurons were observed in the ipsilateral entorhinal cortex and habenula, and contralaterally in the HLDB, VLDB, NBM, thalamus, hypothalamus, and VTA. Bilateral projections also arose from the pontine nucleus and FLM. Numerous FG-positive cells were detected within the *cingulum* (likely to reflect tracer uptake along the injection tract).

Comparative summary of LSN and MSN connectivity

The LSN and MSN share extensive afferent projections from cortical, limbic, diencephalic, and brainstem structures. Common inputs included the prefrontal cortex, IG, anterior olfactory nucleus, BA25, *tenia tecta*, hippocampus, amygdala, thalamus, hypothalamus, VTA, PAG, DSCP, IPN, and RF. However, distinct connectivity patterns differentiated between the two nuclei (Fig. 6). LSN connectivity was characterized by relatively stronger inputs from the brainstem, specifically the RF, raphe nuclei, and mesencephalic structures such as the substantia nigra, as well as hypothalamic regions, including the mammillary bodies, alongside prominent afferents from the amygdalopiriform and piriform cortices. In contrast, MSN connectivity exhibited stronger inputs from the prefrontal cortex and cortical midline structures (BA25, BA33), together with robust reciprocal connections with the VLDB, HLDB, and NBM. While hippocampal projections were consistently bilateral for both nuclei, they were notably more prominent in the MSN. Furthermore, the MSN displayed a higher degree of bilateral organization overall, whereas LSN projections showed greater lateralization. Although occasional tracer uptake was observed along the injection tract, it did not obscure the general connectivity patterns.

DISCUSSION

This study provides a comprehensive cytoarchitectural and retrograde tract-tracing analysis of the GM septal area, establishing a structural framework

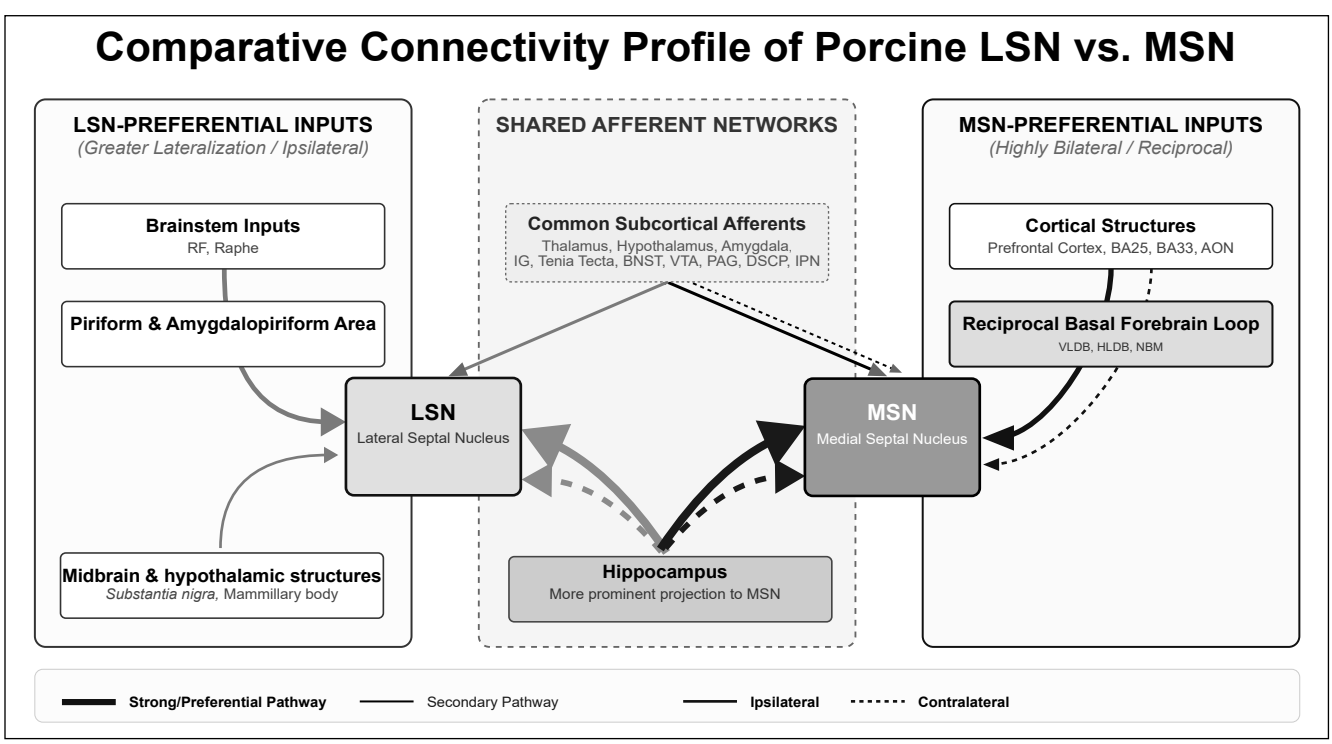

Fig. 6. Schematic diagram summarizing the comparative afferent connectivity of the LSN and MSN. Abbreviations: AON, anterior olfactory nucleus; BA25, Brodmann area 25 homologue; BA33, Brodmann area 33 homologue; BNST, bed nucleus of the stria terminalis; DSCP, decussation of the superior cerebellar peduncle; HLDB, horizontal limb of the diagonal band of Broca; IG, indusium griseum; IPN, interpeduncular nucleus; LSN, lateral septal nucleus; MSN, medial septal nucleus; NBM, nucleus basalis of Meynert; PAG, periaqueductal gray; RF, reticular formation; VLDB, vertical limb of the diagonal band of Broca; VTA, ventral tegmental area.

that fills a critical gap in large-animal neuroanatomy. Previous reports often treated the porcine septum as a single structure (Jelsing et al., 2006; Kornum et al., 2010; Pardo et al., 2021) or divided it into medial and lateral complexes (Bjarkam, Glud, et al., 2017; Mahady et al., 2017). A more detailed description was available for the large white pigs (Felix et al., 1999), though without tract-tracing data.

Macroscopically, the GM septum is a thin, elongated midline structure extending dorsally into a distinct *septum pellucidum*, which separates the large lateral ventricles (Fig. 2e, f). This organization is similar to that of human and non-human primate anatomy (Andy & Stephan, 1968), while differing markedly from the broader septal structure with proportionally smaller lateral ventricles seen in rodents (Andy & Stephan, 1961; Swanson & Cowan, 1979; Radtke-Schuller et al., 2016; Swanson, 2018; Schröder et al., 2020). The *septum pellucidum*, which is absent in rodents, is clearly identifiable in the GM brain (Fig. 2e, f), despite earlier reports suggesting its presence only in higher primates (Andy & Stephan, 1968). This finding is similar to the neuroanatomy of other mammals with larger, gyrencephalic brains, such as fellow ungulates (Nitzsche et al., 2015; Kose & Duzler, 2023) or cetaceans (Avelino-de-Souza et al., 2024), although in certain groups, like carnivores, the *septum pellucidum* is not clearly visible as a thin tissue membrane (De Rycke et al., 2005).

Structurally, our findings demonstrate that the GM septal region is organized into highly differentiated medial, lateral, posterior, and ventral complexes, and, together with the diagonal band of Broca, is conserved across mammals (Andy & Stephan, 1968; Imam et al., 2022; Kumazawa-Manita et al., 2018; Radtke-Schuller, 2018; Risold, 2004; Risold & Swanson, 1997a; Scalia, 2013; Swanson & Cowan, 1979). However, microanatomical details vary among species (Montagnese et al., 2004). The relative size of the septal region in GM is smaller than in rodents or bats but larger than in primates, including humans. This structural preservation validates the GM as an anatomically relevant transitional model between rodent foundational circuitry and human macro-anatomy.

Our finding that the Göttingen minipig septal area is clearly organized into four distinct anatomical subdivisions aligns well with classic mammalian architecture. However, navigating how these subregions are defined in the wider literature highlights the practical impact of the species-specific naming conventions often encountered in comparative mapping. While rodent frameworks identify a highly compartmentalized lateral and posterior septal complex containing the lateral septal nucleus (LSN), the septofimbrial nucleus (SF), the septohippocampal nucleus, the bed nucleus of the stria medullaris (BNSM), and the bed nucleus of the anterior commissure (BNAC) (Risold, 2004; Swanson & Cowan, 1979), alternative digital reference schemas classify structures like the BNAC within the pallidum, grouping them alongside components of the extended amygdala, such as parts of the bed nucleus of the stria terminalis (Sunkin et al., 2013). Though rodent work demonstrates that the BNAC innervates substance P-ergic pathways to the medial habenula to modulate specific motivational, hedonic, and fear responses (Lee et al., 2019), neither the BNAC nor the BNSM could be definitively delineated in our minipig material.

Histologically, the GM medial septal complex contained sparse, large cholinergic neurons within MSN and VLDB, comparable to those observed in humans and rodents. The cytoarchitectural variations and cell body morphologies observed across these subnuclei closely match previous porcine data (Mahady et al., 2017), although they differ from earlier rodent descriptions (Mesulam et al., 1983). We identified multipolar neurons within the MSN, smaller neurons within the HLDB, and multipolar cells within the NBM, confirming previous reports (Mahady et al., 2017), though we did not observe the distinct spindle-shaped neurons described in rodent homologous structures (Swanson & Cowan, 1979; Swanson, 2018). Crucially, our finding that the LSN lacks cholinergic neurons contradicts a previous porcine study (Mahady et al., 2017). Nevertheless, dense cholinergic fibers were present, consistent with known retrograde connectivity patterns. This variance likely stems from methodological factors, such as antibody lot variability or protocol sensitivity. Our protocol generated minimal background artifacts, minimizing the risk of false-positive neuronal classification. However, further studies are needed to confirm this observation.

The tripartite subdivision of the LSN (dorsal, intermediate, and ventral groups) identified here aligns with mammalian architecture (Andy & Stephan, 1968; Swanson & Cowan, 1979). In rodents, detailed histochemical and molecular studies using in situ hybridization and immunohistochemical markers have shown that the LSN can be further subdivided into rostral, caudal, and ventral parts, comprising up to 30 distinct regions (Risold & Swanson, 1997a). The ventral part of the LSN corresponds to the ventral group and contains estrogen receptors (Hasunuma et al., 2024), whereas the rostral and caudal regions described by Risold & Swanson (1997a) correspond topographically to the dorsal and intermediate groups, identified by Nissl staining.

Further studies employing immunohistochemical staining and/or in situ hybridization techniques targeting somatostatin, enkephalin, and estrogen recep-

tors would enable a more detailed anatomical delineation of the GM LSN (Risold & Swanson, 1997a).

Similar to observations in rodents and humans, the septofimbrial nucleus in the Göttingen minipig shares close structural boundaries with the lateral septal nucleus (LSN), acting as a key component of downstream septal circuitry. The septohippocampal nucleus, well-documented in several mammalian species (Swanson & Cowan, 1979; Risold, 2004; Radtke-Schuller et al., 2016; Radtke-Schuller, 2018; Imam et al., 2022), including non-human primates (Iriki et al., 2019; Ragen et al., 2015), and humans (Ding et al., 2016), was not identified in our material. In species where it is present, this small, cytoarchitecturally distinct structure extends rostrocaudally along the dorsal septum toward the hippocampal rudiment. While its precise functional role remains poorly understood, rodent models characterize it as a part of the limbic system that receives hippocampal inputs and contains many somatostatin- and neuropeptide Y-expressing neurons (Risold & Swanson, 1997b; Paxinos, 2015).

The posterior septal complex of the GM includes the triangular nucleus, a conserved mammalian structure (Swanson & Cowan, 1979; Ding et al., 2016; Iriki et al., 2019). This nucleus extends from the BNST along the ventral fimbria toward the hippocampus (Scalia, 2013; Radtke-Schuller, 2018; Imam et al., 2022). The BNST has been described in detail in numerous mammalian species (Swanson & Cowan 1979; Felix et al. 1999; Ettrup et al. 2010; Bjarkam et al. 2017a; Swanson, 2018) and is often referred to as part of the extended amygdala. It contains predominantly GABAergic neurons, but also a subset of cholinergic cells (Mai & Paxinos, 2012; Mahady et al., 2017; Maita et al., 2021). This compact, yet heterogeneous nucleus exhibits sexual dimorphism and can be divided into numerous subnuclei (Ding, 2023) - up to eighteen in the rat (Bota et al., 2012). Although we identified the BNST in the GM, further parcellation is needed.

In agreement with other pig brain studies (Felix et al., 1999; Bjarkam, Glud, et al., 2017) we did not identify the BNSM, a small, enkephalin-positive nucleus present in rodents and located medially to the stria medullaris near the stria terminalis (Andy & Stephan, 1961; Swanson & Cowan, 1979; Risold & Swanson, 1995, 1997a; Risold, 2004). The nucleus of the stria medullaris has also been described in pangolins (Imam et al., 2022), and its presence in humans remains uncertain, with some studies reporting it (Andy & Stephan, 1968), while others do not (Ding et al., 2016).

Our findings regarding the HLDB and NBM broadly agree with those of Mahady et al. (2017). According to Mesulam et al. (1983), the NSM, VLDB, HLDB, and NBM correspond to the cholinergic nuclei CH1-CH4. Morphological transitions between these nuclei were apparent: the boundary between NSM and VLDB corresponded to a reduction in cell size, while between VLDB and HLDB, the orientation of cholinergic neurons shifted. The internal capsule delineated the HLDB-NBM transition, coinciding with greater dispersion of the cholinergic neurons and the appearance of larger multipolar cells (Mahady et al., 2017).

The BNAC was not identified in the GM, although it has been described in other mammals, including rodents and primates (Davis et al., 1968; Risold, 2004; Radtke-Schuller et al., 2016; Iriki et al., 2019; Iyer & Tole, 2020; Imam et al., 2022) and in earlier studies of the human brain (Andy & Stephan, 1968). However, it is not mentioned in recent human atlases such as the Allen Human Brain Atlas or The Human Nervous System (Mai & Paxinos, 2012; Ding et al., 2016). Similarly, the interstitial nucleus of the posterior limb of the anterior commissure (IPAC), described as a part of the extended amygdala in humans (Mai et al., 2016), was likewise not observed in our material. Prior studies suggest that IPAC and BNAC/BAC are distinct entities (Shammah-Lagnado et al., 2001; Risold, 2004).

Rather than reflecting an evolutionary divergence in porcine brain wiring, the apparent absence of these subtle micro-nuclei (septohippocampal nucleus, IPAC, BNSM, and BNAC) in our study most likely is a result of technical constraints. The use of relatively coarse sectioning (800 µm intervals) may have caused omission of these very small nuclei, and their cytoarchitecture on Nissl stains closely resembles that of adjacent regions, complicating identification (Fig. 2i). To address these limitations, future investigations should employ denser sectioning combined with immunohistochemical or in situ hybridization approaches targeting specific markers like somatostatin or estrogen receptors to improve visualization of these small, cytoarchitecturally subtle boundaries.

Despite subtle variations in cholinergic localization and the apparent absence of a few small nuclei, like IPAC, BNSM, and BNAC, the GM exhibits a highly conserved septal organization. This structural homology is particularly noteworthy because the medial septum and diagonal band complex constitute the main source of cholinergic innervation to the hippocampus (Mesulam et al., 1983; Magno et al., 2017; Muller & Remy, 2018). These structures are essential for driving septo-hippocampal oscillations, learning, and memory. Consequently, our mapping of this pathway provides an anatomical framework for evaluating these structures as therapeutic targets in clinical conditions associated with pathological network oscillations, such as epilepsy, affective disorders, and Alzheimer's disease (Jeong et al., 2014; Takeuchi et al., 2021; He et al., 2023). Our

retrograde tracing experiment successfully maps the afferent projections to the GM LSN and MSN (Table 1), revealing a complex network of subcortical and cortical inputs that match patterns predicted by the rodent literature. These distinct pathways align closely with conserved mammalian functional systems, where the structural divisions of the lateral septal complex are known to integrate widespread limbic inputs to regulate states of fear, aggression, and motivation (Iyer & Tole, 2020; Patel, 2022; Puska et al., 2024). Both the LSN and MSN received inputs from the PAG, IPN, VTA, hypothalamus, thalamus, and amygdala, with strong internal projections from LSN to MSN. However, the LSN showed stronger projections from brainstem regions such as RF and RN, whereas the MSN received stronger input from the prefrontal cortex and the anterior olfactory nucleus. The prominent inputs observed from the amygdala and hypothalamus to the minipig LSC are consistent with this functional framework. Furthermore, while the posterior septal complex, specifically the triangular nucleus, was successfully identified, its companion structure, the BNAC, was not. In rodent models, the posterior septal nuclei project directly to the medial habenula, forming a distinct substance P-ergic pathway implicated in anxiety, stress regulation, and reward-related behaviors (Yamaguchi et al., 2013; Otsu et al., 2018; Lee et al., 2019).

In rats, the LSN receives projections from the hippocampus, hypothalamus, RF, substantia nigra, PAG, and SCN. Anterograde tracing studies further showed projections to the *tenia tecta*, *zona incerta*, DSCP, IPN, MSN, VLDB, HLDB, thalamus, and amygdala (Swanson & Cowan, 1979; Sorensen et al., 1993; Risold & Swanson, 1997b; Oh et al., 2014). As our findings indicate, the hippocampal and hypothalamic inputs to the LSN are bilateral. These connections are not only relevant for septohippocampal modulation of memory processes but also for social behavior. For example, studies in mice demonstrated that hippocampal projections from the CA2 area to the dorsal LSN promote social aggression (Leroy et al., 2018). Another tracing study using rats showed that the medial septum receives connections from the *nucleus incertus*, while the raphe nuclei project to the posterior septal complex (Sanchez-Perez et al., 2015; Gil-Miravet et al., 2023).

The structural and connectional similarities observed between the minipig MSN-VLDB continuum, the HLDB, and the NBM suggest that the fundamental layout of the basal forebrain cholinergic projection system to the hippocampus is maintained in this model (Magno et al., 2017; Muller & Remy, 2018). Tracings to the MSN in rats have found projections from NBM, HLDB, VLDB, hypothalamus, and *tenia tecta* (Swanson & Cowan, 1979). These connections were originally described by injecting these nuclei with an anterograde tracer and describing the distribution. Therefore, identified connections are restricted to the nuclei targeted by injection and do not encompass the full range of septal connectivity. Nonetheless, they correspond well with our results derived from retrograde tracing following tracer administration into MSN, supporting the value of the Göttingen minipig as a relevant model for studying the structural organization and function of the mammalian septum (Sørensen et al., 2011).

The retrograde connections of the MSN and LSN in the GM have now been described in detail. However, the connectivity of the ventral and posterior septal complexes, as well as other nuclei within the medial and lateral septal complexes, remains undescribed, as these areas were not targeted in the present study. Likewise, anterograde projections could not be delineated, as unsuccessful BDA tracing prevented visualization of efferent pathways from the LSN and MSN.

Several methodological considerations should guide the interpretation of these connectivity results. For instance, variable tracer leakage into the tissue bordering the lateral ventricles may have introduced potential confounding signals. Similarly, FG-positive cells observed in the cingulum and cortex of PIG01 and PIG06 likely reflect tracer uptake along the injection tract rather than true retrograde connections. This technical variability accounts for the inter-animal differences in total labeled nuclei observed across our cohort. Furthermore, the technical failure of the BDA anterograde tracing restricted our analysis to afferent pathways. While some small, isolated axon-like profiles were visible, they could not, except in some isolated regions, such as the hypothalamus or amygdala, be reliably distinguished from background tissue artifacts and were therefore excluded from the final analysis to preserve data integrity.

Another factor concerns immunohistochemical variability. Discrepancies in the distribution of cholinergic neurons between our study and that of Mahady et al. (2017) may reflect differences in antibody batches or staining protocols. Our protocol produced lower background staining, which may have reduced the risk of false-positive neuronal identification. Future studies incorporating additional neurochemical markers (e.g., somatostatin, enkephalin, or calbindin) will help refine the anatomical delineation of septal subnuclei and confirm cholinergic localization. Despite these limitations, the retrograde labeling observed in our study confirms that the fundamental wiring of the GM septal area is similar to that of the human and rodent basal forebrain, supporting its potential implementation in translational models of human neurological disease.

CONCLUSIONS

This study demonstrates that the Göttingen minipig possesses a highly differentiated septal region that shares key structural and connectional features with those of rodents and primates. Our findings describe the organization of the minipig septal area into four distinct complexes: the medial, lateral, ventral, and posterior septal complexes. In line with observations in other mammalian species, the medial septal complex contains a population of cholinergic neurons. These anatomical similarities suggest that the Göttingen minipig may serve as a useful large-animal model for studying septal and basal forebrain circuitry, potentially aiding the future exploration of therapeutic approaches for related neurodegenerative conditions, such as Alzheimer's disease.

ACKNOWLEDGMENTS

The authors would like to thank Trine W. Mikkelsen for histotechnical assistance, Lise Moberg Fitting, and Anne Sofie Møller Andersen for administrative support. Thank you to the staff of the animal facility at Påskehøjgaard. The Danish Neurosurgical Society, Lundbeck Fonden, and A.P. Møller Fonden financially supported the study.

REFERENCES

Andy, O. J., & Stephan, H. (1961). Septal nuclei in the Soricidae (insectivors). Cyto-architectonic study. *J Comp Neurol*, *117*, 251–273. https://doi.org/10.1002/cne.901170211

Andy, O. J., & Stephan, H. (1968). The septum in the human brain. *J Comp Neurol*, *133*(3), 383–410. https://doi.org/10.1002/cne.901330308

Avelino-de-Souza, K., Mynssen, H., Chaim, K., Parks, A. N., Ikeda, J. M. P., Cunha, H. A., Mota, B., & Patzke, N. (2024). Anatomical and volumetric description of the guiana dolphin (Sotalia guianensis) brain from an ultra-high-field magnetic resonance imaging. *Brain Struct Funct*, *229*(8), 1889–1911. https://doi.org/10.1007/s00429-024-02789-1

Bech, J., Orlowski, D., Glud, A. N., Dyrby, T. B., Sorensen, J. C. H., & Bjarkam, C. R. (2020). Ex vivo diffusion-weighted MRI tractography of the Gottingen minipig limbic system. *Brain Struct Funct*, *225*(3), 1055–1071. https://doi.org/10.1007/s00429-020-02058-x

Bjarkam, C. R., Cancian, G., Larsen, M., Rosendahl, F., Ettrup, K. S., Zeidler, D., Blankholm, A. D., Ostergaard, L., Sunde, N., & Sorensen, J. C. (2004). A MRI-compatible stereotaxic localizer box enables high-precision stereotaxic procedures in pigs. *J Neurosci Methods*, *139*(2), 293–298. https://doi.org/10.1016/j.jneumeth.2004.05.004

Bjarkam, C. R., Glud, A. N., Orlowski, D., Sorensen, J. C. H., & Palomero-Gallagher, N. (2017). The telencephalon of the Gottingen minipig, cytoarchitecture and cortical surface anatomy. *Brain Struct Funct*, *222*(5), 2093–2114. https://doi.org/10.1007/s00429-016-1327-5

Bjarkam, C. R., Jorgensen, R. L., Jensen, K. N., Sunde, N. A., & Sorensen, J. C. (2008). Deep brain stimulation electrode anchoring using BioGlue((R)), a protective electrode covering, and a titanium microplate. *J Neurosci Methods*, *168*(1), 151–155. https://doi.org/10.1016/j.jneumeth.2007.09.008

Bjarkam, C. R., Orlowski, D., Tvilling, L., Bech, J., Glud, A. N., & Sorensen, J. H. (2017). Exposure of the Pig CNS for Histological Analysis: A Manual for Decapitation, Skull Opening, and Brain Removal. *J Vis Exp*, *2017*(122), Article e55511. https://doi.org/10.3791/55511

Bjarkam, C. R., Pedersen, M., & Sorensen, J. C. (2001). New strategies for embedding, orientation and sectioning of small brain specimens enable direct correlation to MR-images, brain atlases, or use of unbiased stereology. *J Neurosci Methods*, *108*(2), 153–159. https://doi.org/10.1016/s0165-0270(01)00383-1

Christensen, A. B., Sorensen, J. C. H., Ettrup, K. S., Orlowski, D., & Bjarkam, C. R. (2018). Pirouetting pigs: A large non-primate animal model based on unilateral 6-hydroxydopamine lesioning of the nigrostriatal pathway. *Brain Res Bull*, *139*, 167–173. https://doi.org/10.1016/j.brainresbull.2018.02.010

Cruz, M. L., & Beyer, C. (1972). Effects of septal lesions on maternal behavior and lactation in the rabbit. *Physiol Behav*, *9*(3), 361–365. https://doi.org/10.1016/0031-9384(72)90160-6

Danielsen, E. H., Cumming, P., Andersen, F., Bender, D., Brevig, T., Falborg, L., Gee, A., Gillings, N. M., Hansen, S. B., Hermansen, F., Johansen, J., Johansen, T. E., Dahl-Jorgensen, A., Jorgensen, H. A., Meyer, M., Munk, O., Pedersen, E. B., Poulsen, P. H., Rodell, A. B.,...Moller, A. (2000). The DaNeX study of embryonic mesencephalic, dopaminergic tissue grafted to a minipig model of Parkinson's disease: preliminary findings of effect of MPTP poisoning on striatal dopaminergic markers. *Cell Transplant*, *9*(2), 247–259. https://doi.org/10.1177/096368970000900210

Davis, R., Huffman, R. D., Southwest Foundation for, R., & Education. (1968). *A stereotaxic atlas of the brain of the baboon (Papio)*. Published for the Southwest Foundation for Research and Education by the University of Texas Press Austin.

De Rycke, L. M., Gielen, I. M., Van Meervenne, S. A., Simoens, P. J., & van Bree, H. J. (2005). Computed tomography and cross-sectional anatomy of the brain in clinically normal dogs. *American Journal of Veterinary Research*, *66*(10), 1743–1756. https://doi.org/DOI 10.2460/ajvr.2005.66.1743

Ding, S. L., Royall, J. J., Sunkin, S. M., Ng, L., Facer, B. A., Lesnar, P., Guillozet-Bongaarts, A., McMurray, B., Szafer, A., Dolbeare, T. A., Stevens, A., Tirrell, L., Benner, T., Caldejon, S., Dalley, R. A., Dee, N., Lau, C., Nyhus, J., Reding, M.,...Lein, E. S. (2016). Comprehensive cellular-resolution atlas of the adult human brain. *J Comp Neurol*, *524*(16), 3127–3481. https://doi.org/10.1002/cne.24080

Dolezalova, D., Hruska-Plochan, M., Bjarkam, C. R., Sorensen, J. C., Cunningham, M., Weingarten, D., Ciacci, J. D., Juhas, S., Juhasova, J., Motlik, J., Hefferan, M. P., Hazel, T., Johe, K., Carromeu, C., Muotri, A., Bui, J., Strnadel, J., & Marsala, M. (2014). Pig models of neurodegenerative disorders: Utilization in cell replacement-based preclinical safety and efficacy studies. *J Comp Neurol*, *522*(12), 2784–2801. https://doi.org/10.1002/cne.23575

Ettrup, K. S., Glud, A. N., Orlowski, D., Fitting, L. M., Meier, K., Soerensen, J. C., Bjarkam, C. R., & Alstrup, A. K. (2011). Basic surgical techniques in the Gottingen minipig: intubation, bladder catheterization, femoral vessel catheterization, and transcardial perfusion . *J Vis Exp*(52), Article e2652. https://doi.org/10.3791/2652

Ettrup, K. S., Sorensen, J. C., & Bjarkam, C. R. (2010). The anatomy of the Gottingen minipig hypothalamus. *J Chem Neuroanat*, *39*(3), 151–165. https://doi.org/10.1016/j.jchemneu.2009.12.004

Ettrup, K. S., Sorensen, J. C., Rodell, A., Alstrup, A. K., & Bjarkam, C. R. (2012). Hypothalamic deep brain stimulation influences autonomic and limbic circuitry involved in the regulation of aggression and cardiocerebrovascular control in the Gottingen minipig . *Stereotact Funct Neurosurg*, *90*(5), 281–291. https://doi.org/10.1159/000338087

Felix, B., Leger, M. E., Albe-Fessard, D., Marcilloux, J. C., Rampin, O., & Laplace, J. P. (1999). Stereotaxic atlas of the pig brain. *Brain Res Bull*, *49*(1-2), 1–137. https://doi.org/10.1016/s0361-9230(99)00012-x

Fisher, R. S. (2015). Stimulation of the medial septum should benefit patients with temporal lobe epilepsy. *Med Hypotheses*, *84*(6), 543–550. https://doi.org/10.1016/j.mehy.2015.02.016

Gil-Miravet, I., Nunez-Molina, A., Navarro-Sanchez, M., Castillo-Gomez, E., Ros-Bernal, F., Gundlach, A. L., & Olucha-Bordonau, F. E. (2023). Nucleus incertus projections to rat medial septum and entorhinal cortex: rare collateralization and septal-gating of temporal lobe theta rhythm activity. *Brain Struct Funct*, *228*(5), 1307–1328. https://doi.org/10.1007/s00429-023-02650-x

Glud, A. N., Bech, J., Tvilling, L., Zaer, H., Orlowski, D., Fitting, L. M., Ziedler, D., Geneser, M., Sangill, R., Alstrup, A. K. O., Bjarkam, C. R., & Sorensen, J. C. H. (2017). A fiducial skull marker for precise MRI-based stereotaxic surgery in large animal models. *J Neurosci Methods*, *285*, 45–48. https://doi.org/10.1016/j.jneumeth.2017.04.017

Glud, A. N., Bjarkam, C. R., Azimi, N., Johe, K., Sorensen, J. C., & Cunningham, M. (2016). Feasibility of Three-Dimensional Placement of Human Therapeutic Stem Cells Using the Intracerebral Microinjection Instrument. *Neuromodulation*, *19*(7), 708–716. https://doi.org/10.1111/ner.12484

Glud, A. N., Zaer, H., Orlowski, D., Nielsen, M. S., Sorensen, J. C. H., & Bjarkam, C. R. (2024). Anatomy and connectivity of the Gottingen minipig subgenual cortex (Brodmann area 25 homologue). *Brain Struct Funct*, *229*(8), 1995–2010. https://doi.org/10.1007/s00429-024-02855-8

Hasunuma, K., Murakawa, T., Takenawa, S., Mitsui, K., Hatsukano, T., Sano, K., Nakata, M., & Ogawa, S. (2024). Estrogen Receptor beta in the Lateral Septum Mediates Estrogen Regulation of Social Anxiety-like Behavior in Male Mice. *Neuroscience*, *537*, 126–140. https://doi.org/10.1016/j.neuroscience.2023.11.019

He, G., Li, Y., Deng, H., & Zuo, H. (2023). Advances in the study of cholinergic circuits in the central nervous system. *Ann Clin Transl Neurol*, *10*(12), 2179–2191. https://doi.org/10.1002/acn3.51920

Imam, A., Bhagwandin, A., Ajao, M. S., & Manger, P. R. (2022). The brain of the tree pangolin (Manis tricuspis). VIII. The subpallial telencephalon. *J Comp Neurol*, *530*(15), 2611–2644. https://doi.org/10.1002/cne.25353

Iriki, A., Okano, H. J., Sasaki, E., & Okano, H. (2019). *The 3-dimensional atlas of the marmoset brain : reconstructible in stereotaxic coordinates*. Springer Tokyo.

Iyer, A., & Tole, S. (2020). Neuronal diversity and reciprocal connectivity between the vertebrate hippocampus and septum. *Wiley Interdiscip Rev Dev Biol*, *9*(4), e370. https://doi.org/10.1002/wdev.370

Jelsing, J., Hay-Schmidt, A., Dyrby, T., Hemmingsen, R., Uylings, H. B., & Pakkenberg, B. (2006). The prefrontal cortex in the Gottingen minipig brain defined by neural projection criteria and cytoarchitecture. *Brain Res Bull*, *70*(4-6), 322–336. https://doi.org/10.1016/j.brainresbull.2006.06.009

Jeong, D. U., Lee, J. E., Lee, S. E., Chang, W. S., Kim, S. J., & Chang, J. W. (2014). Improvements in memory after medial septum stimulation are associated with changes in hippocampal cholinergic activity and neurogenesis. *Biomed Res Int*, *2014*, 568587. https://doi.org/10.1155/2014/568587

Kamali, A., Milosavljevic, S., Gandhi, A., Lano, K. R., Shobeiri, P., Sherbaf, F. G., Sair, H. I., Riascos, R. F., & Hasan, K. M. (2023). The Cortico-Limbo-Thalamo-Cortical Circuits: An Update to the Original Papez Circuit of the Human Limbic System. *Brain Topogr*, *36*(3), 371–389. https://doi.org/10.1007/s10548-023-00955-y

Kornum, B. R., Stott, S. R., Mattsson, B., Wisman, L., Ettrup, A., Hermening, S., Knudsen, G. M., & Kirik, D. (2010). Adeno-associated viral vector serotypes 1 and 5 targeted to the neonatal rat and pig striatum induce widespread transgene expression in the forebrain. *Exp Neurol*, *222*(1), 70–85. https://doi.org/10.1016/j.expneurol.2009.12.009

Kose, F., & Duzler, A. (2023). An anatomical and volumetric study on brain ventricles in sheep using different techniques. *Anat Histol Embryol*, *52*(5), 732–741. https://doi.org/10.1111/ahe.12930

Kumazawa-Manita, N., Hashikawa, T., & Iriki, A. (2018). *The 3D stereotaxic brain atlas of the degu : with MRI and histology digital model with a freely rotatable viewer*. Springer Tokyo, Japan. https://doi.org/10.1007/978-4-431-56615-1

Larsen, M., Bjarkam, C. R., Ostergaard, K., West, M. J., & Sorensen, J. C. (2004). The anatomy of the porcine subthalamic nucleus evaluated with immunohistochemistry and design-based stereology. *Anat Embryol (Berl)*, *208*(3), 239–247. https://doi.org/10.1007/s00429-004-0395-0

Lee, H. W., Yang, S. H., Kim, J. Y., & Kim, H. (2019). The Role of the Medial Habenula Cholinergic System in Addiction and Emotion-Associated Behaviors. *Front Psychiatry*, *10*, 100. https://doi.org/10.3389/fpsyt.2019.00100

Leroy, F., Park, J., Asok, A., Brann, D. H., Meira, T., Boyle, L. M., Buss, E. W., Kandel, E. R., & Siegelbaum, S. A. (2018). A circuit from hippocampal CA2 to lateral septum disinhibits social aggression. *Nature*, *564*(7735), 213–218. https://doi.org/10.1038/s41586-018-0772-0

Lind, N. M., Moustgaard, A., Jelsing, J., Vajta, G., Cumming, P., & Hansen, A. K. (2007). The use of pigs in neuroscience: modeling brain disorders. *Neurosci Biobehav Rev*, *31*(5), 728–751. https://doi.org/10.1016/j.neubiorev.2007.02.003

Magno, L., Barry, C., Schmidt-Hieber, C., Theodotou, P., Hausser, M., & Kessaris, N. (2017). NKX2-1 Is Required in the Embryonic Septum for Cholinergic System Development, Learning, and Memory. *Cell Rep*, *20*(7), 1572–1584. https://doi.org/10.1016/j.celrep.2017.07.053

Mahady, L. J., Perez, S. E., Emerich, D. F., Wahlberg, L. U., & Mufson, E. J. (2017). Cholinergic profiles in the Goettingen miniature pig (Sus scrofa domesticus) brain. *J Comp Neurol*, *525*(3), 553–573. https://doi.org/10.1002/cne.24087

Mai, J. r. K., Majtanik, M., & Paxinos, G. (2016). *Atlas of the human brain* (4th edition ed.). Academic Press, an imprint of Elsevier Amsterdam.

Mai, J. r. K., & Paxinos, G. (2012). *The human nervous system* (3rd ed.). Elsevier Academic Press.

Maita, I., Bazer, A., Blackford, J. U., & Samuels, B. A. (2021). Functional anatomy of the bed nucleus of the stria terminalis-hypothalamus neural circuitry: Implications for valence surveillance, addiction, feeding, and social behaviors. *Handb Clin Neurol*, *179*, 403–418. https://doi.org/10.1016/B978-0-12-819975-6.00026-1

Meidahl, A. C., Orlowski, D., Sorensen, J. C., & Bjarkam, C. R. (2016). The Retrograde Connections and Anatomical Segregation of the Gottingen Minipig Nucleus Accumbens. *Front Neuroanat*, *10*, 117. https://doi.org/10.3389/fnana.2016.00117

Melia-Sorolla, M., Castano, C., DeGregorio-Rocasolano, N., Rodriguez--Esparragoza, L., Davalos, A., Marti-Sistac, O., & Gasull, T. (2020). Relevance of Porcine Stroke Models to Bridge the Gap from Pre-Clinical Findings to Clinical Implementation. *Int J Mol Sci*, *21*(18). https://doi.org/10.3390/ijms21186568

Mesulam, M. M., Mufson, E. J., Wainer, B. H., & Levey, A. I. (1983). Central cholinergic pathways in the rat: an overview based on an alternative nomenclature (Ch1-Ch6). *Neuroscience*, *10*(4), 1185–1201. https://doi.org/10.1016/0306-4522(83)90108-2

Meza, E., Aguirre, J., Waliszewski, S., & Caba, M. (2015). Suckling induces a daily rhythm in the preoptic area and lateral septum but not in the bed nucleus of the stria terminalis in lactating rabbit does. *Eur J Neurosci*, *41*(2), 196–204. https://doi.org/10.1111/ejn.12776

Montagnese, C. M., Szekely, A. D., Adam, A., & Csillag, A. (2004). Efferent connections of septal nuclei of the domestic chick (Gallus domesticus): an anterograde pathway tracing study with a bearing on functional circuits. *J Comp Neurol*, *469*(3), 437–456. https://doi.org/10.1002/cne.11018

Montagnese, C. M., Zachar, G., Balint, E., & Csillag, A. (2008). Afferent connections of septal nuclei of the domestic chick (Gallus domesticus): a retrograde pathway tracing study. *J Comp Neurol*, *511*(1), 109–150. https://doi.org/10.1002/cne.21837

Muller, C., & Remy, S. (2018). Septo-hippocampal interaction. *Cell Tissue Res*, *373*(3), 565–575. https://doi.org/10.1007/s00441-017-2745-2

Nitzsche, B., Frey, S., Collins, L. D., Seeger, J., Lobsien, D., Dreyer, A., Kirsten, H., Stoffel, M. H., Fonov, V. S., & Boltze, J. (2015). A stereotaxic, population-averaged T1w ovine brain atlas including cerebral morphol-

ogy and tissue volumes. *Front Neuroanat*, *9*, 69. https://doi.org/10.3389/fnana.2015.00069

Numan, R. (2000). *The behavioral neuroscience of the septal region*. Springer New York. https://doi.org/10.1007/978-1-4612-1302-4

Oh, S. W., Harris, J. A., Ng, L., Winslow, B., Cain, N., Mihalas, S., Wang, Q., Lau, C., Kuan, L., Henry, A. M., Mortrud, M. T., Ouellette, B., Nguyen, T. N., Sorensen, S. A., Slaughterbeck, C. R., Wakeman, W., Li, Y., Feng, D., Ho, A.,... Zeng, H. (2014). A mesoscale connectome of the mouse brain. *Nature*, *508*(7495), 207–214. https://doi.org/10.1038/nature13186

Orlowski, D., Glud, A. N., Palomero-Gallagher, N., Sorensen, J. C. H., & Bjarkam, C. R. (2019). Online histological atlas of the Gottingen minipig brain. *Heliyon*, *5*(3), e01363. https://doi.org/10.1016/j.heliyon.2019.e01363

Orlowski, D., Michalis, A., Glud, A. N., Korshoj, A. R., Fitting, L. M., Mikkelsen, T. W., Mercanzini, A., Jordan, A., Dransart, A., & Sorensen, J. C. H. (2017). Brain Tissue Reaction to Deep Brain Stimulation-A Longitudinal Study of DBS in the Goettingen Minipig. *Neuromodulation*, *20*(5), 417–423. https://doi.org/10.1111/ner.12576

Otsu, Y., Lecca, S., Pietrajtis, K., Rousseau, C. V., Marcaggi, P., Dugue, G. P., Mailhes-Hamon, C., Mameli, M., & Diana, M. A. (2018). Functional Principles of Posterior Septal Inputs to the Medial Habenula. *Cell Rep*, *22*(3), 693–705. https://doi.org/10.1016/j.celrep.2017.12.064

Pardo, I. D., Manno, R. A., Capobianco, R., Sargeant, A. M., Morrison, J. P., Bolon, B., & Garman, R. H. (2021). Nervous System Sampling for General Toxicity and Neurotoxicity Studies in the Laboratory Minipig With Emphasis on the Gottingen Minipig. *Toxicol Pathol*, *49*(6), 1140–1163. https://doi.org/10.1177/01926233211019941

Parent, A., & O'Reilly-Fromentin, J. (1982). Distribution and morphological characteristics of acetylcholinesterase-containing neurons in the basal forebrain of the cat. *Brain Res Bull*, *8*(2), 183–196. https://doi.org/10.1016/0361-9230(82)90045-4

Patel, H. (2022). The role of the lateral septum in neuropsychiatric disease. *J Neurosci Res*, *100*(7), 1422–1437. https://doi.org/10.1002/jnr.25052

Paxinos, G. (2015). *The rat nervous system* (Fourth edition ed.). Elsevier/Academic Press.

Pompolo, S., Ischenko, O., Pereira, A., Iqbal, J., & Clarke, I. J. (2005). Evidence that projections from the bed nucleus of the stria terminalis and from the lateral and medial regions of the preoptic area provide input to gonadotropin releasing hormone (GNRH) neurons in the female sheep brain. *Neuroscience*, *132*(2), 421–436. https://doi.org/10.1016/j.neuroscience.2004.12.042

Poulsen, A., Zaer, H., Sogaard, B., Glud, A. N., Sorensen, J. C. H., & Orlowski, D. (2026). The neuroanatomy and connectivity of the ventral striatum and ventral capsule area in the Gottingen minipig. *Brain Struct Funct*, *231*(5). https://doi.org/10.1007/s00429-026-03115-7

Puska, G., Szendi, V., & Dobolyi, A. (2024). Lateral septum as a possible regulatory center of maternal behaviors. *Neurosci Biobehav Rev*, *161*, 105683. https://doi.org/10.1016/j.neubiorev.2024.105683

Radtke-Schuller, S. (2018). *Cyto- and myeloarchitectural brain atlas of the ferret (Mustela putorius) in MRI aided stereotaxic coordinates*. Springer Cham.

Radtke-Schuller, S., Schuller, G., Angenstein, F., Grosser, O. S., Goldschmidt, J., & Budinger, E. (2016). Brain atlas of the Mongolian gerbil (Meriones unguiculatus) in CT/MRI-aided stereotaxic coordinates. *Brain Struct Funct*, *221 Suppl 1*(Suppl 1), 1–272. https://doi.org/10.1007/s00429-016-1259-0

Ragen, B. J., Freeman, S. M., Laredo, S. A., Mendoza, S. P., & Bales, K. L. (2015). mu and kappa opioid receptor distribution in the monogamous titi monkey (Callicebus cupreus): implications for social behavior and endocrine functioning. *Neuroscience*, *290*, 421–434. https://doi.org/10.1016/j.neuroscience.2015.01.023

Risold, P. Y. (2004). The Septal Region. In G. Paxinos (Ed.), *The Rat Nervous System* (pp. 605–632). Academic Press. https://doi.org/10.1016/b978-012547638-6/50021-3

Risold, P. Y., & Swanson, L. W. (1995). Cajal's nucleus of the stria medullaris: characterization by in situ hybridization and immunohistochemistry for enkephalin . *J Chem Neuroanat*, *9*(4), 235–240. https://doi.org/10.1016/0891-0618(95)00083-6

Risold, P. Y., & Swanson, L. W. (1997a). Chemoarchitecture of the rat lateral septal nucleus. *Brain Res Brain Res Rev*, *24*(2-3), 91–113. https://doi.org/10.1016/s0165-0173(97)00008-8

Risold, P. Y., & Swanson, L. W. (1997b). Connections of the rat lateral septal complex. *Brain Res Brain Res Rev*, *24*(2-3), 115–195. https://doi.org/10.1016/s0165-0173(97)00009-x

Roxo, M. R., Franceschini, P. R., Zubaran, C., Kleber, F. D., & Sander, J. W. (2011). The limbic system conception and its historical evolution. *ScientificWorldJournal*, *11*, 2428–2441. https://doi.org/10.1100/2011/157150

Sanchez-Perez, A. M., Arnal-Vicente, I., Santos, F. N., Pereira, C. W., ElMlili, N., Sanjuan, J., Ma, S., Gundlach, A. L., & Olucha-Bordonau, F. E. (2015). Septal projections to nucleus incertus in the rat: bidirectional pathways for modulation of hippocampal function. *J Comp Neurol*, *523*(4), 565–588. https://doi.org/10.1002/cne.23687

Scalia, F. (2013). *Forebrain atlas of the short-tailed fruit bat, carollia perpicillata*. Springer New York.

Schröder, H. r., Moser, N., & Huggenberger, S. (2020). *Neuroanatomy of the mouse : an introduction*. Springer Cham. https://doi.org/10.1007/978-3-030-19898-5

Seminara, S. B., Messager, S., Chatzidaki, E. E., Thresher, R. R., Acierno, J. S., Jr., Shagoury, J. K., Bo-Abbas, Y., Kuohung, W., Schwinof, K. M., Hendrick, A. G., Zahn, D., Dixon, J., Kaiser, U. B., Slaugenhaupt, S. A., Gusella, J. F., O'Rahilly, S., Carlton, M. B., Crowley, W. F., Jr., Aparicio, S. A., & Colledge, W. H. (2003). The GPR54 gene as a regulator of puberty. *N Engl J Med*, *349*(17), 1614–1627. https://doi.org/10.1056/NEJMoa035322

Shammah-Lagnado, S. J., Alheid, G. F., & Heimer, L. (2001). Striatal and central extended amygdala parts of the interstitial nucleus of the posterior limb of the anterior commissure: evidence from tract-tracing techniques in the rat. *J Comp Neurol*, *439*(1), 104–126. https://doi.org/10.1002/cne.1999

Sorensen, J. C., Bjarkam, C. R., Danielsen, E. H., Simonsen, C. Z., & Geneser, F. A. (2000). Oriented sectioning of irregular tissue blocks in relation to computerized scanning modalities: results from the domestic pig brain. *J Neurosci Methods*, *104*(1), 93–98. https://doi.org/10.1016/s0165-0270(00)00330-7

Sorensen, J. C., Grabowski, M., Zimmer, J., & Johansson, B. B. (1996). Fetal neocortical tissue blocks implanted in brain infarcts of adult rats interconnect with the host brain. *Exp Neurol*, *138*(2), 227–235. https://doi.org/10.1006/exnr.1996.0061

Sørensen, J. C., Nielsen, M. S., Rosendal, F., Deding, D., Ettrup, K. S., Jensen, K. N., Jørgensen, R. L., Glud, A. N., Meier, K., Fitting, L. M., Møller, A., Alstrup, A. K. O., Østergaard, L., & Bjarkam, C. R. (2011). Development of neuromodulation treatments in a large animal model-Do neurosurgeons dream of electric pigs? In *Progress in brain research* (Vol. 194, pp. 97–103).

Sorensen, J. C., Tonder, N., & Slomianka, L. (1993). Zinc-positive afferents to the rat septum originate from distinct subpopulations of zinc-containing neurons in the hippocampal areas and layers. A combined fluoro-gold tracing and histochemical study. *Anat Embryol (Berl)*, *188*(2), 107–115. https://doi.org/10.1007/BF00186245

Steinmuller, J. B., Bjarkam, C. R., Orlowski, D., Sorensen, J. C. H., & Glud, A. N. (2021). Anterograde Tracing From the Gottingen Minipig Motor and Prefrontal Cortex Displays a Topographic Subthalamic and Striatal Axonal Termination Pattern Comparable to Previous Findings in Primates. *Front Neural Circuits*, *15*, 716145. https://doi.org/10.3389/fncir.2021.716145

Sunkin, S. M., Ng, L., Lau, C., Dolbeare, T., Gilbert, T. L., Thompson, C. L., Hawrylycz, M., & Dang, C. (2013). Allen Brain Atlas: an integrated spatio-temporal portal for exploring the central nervous system. *Nucleic Acids Res*, *41*(Database issue), D996–D1008. https://doi.org/10.1093/nar/gks1042

Swanson, L. W. (2018). Brain maps 4.0-Structure of the rat brain: An open access atlas with global nervous system nomenclature ontology

and flatmaps. *J Comp Neurol*, *526*(6), 935–943. https://doi.org/10.1002/cne.24381

Swanson, L. W., & Cowan, W. M. (1979). The connections of the septal region in the rat. *J Comp Neurol*, *186*(4), 621–655. https://doi.org/10.1002/cne.901860408

Takeuchi, Y., Nagy, A. J., Barcsai, L., Li, Q., Ohsawa, M., Mizuseki, K., & Berenyi, A. (2021). The Medial Septum as a Potential Target for Treating Brain Disorders Associated With Oscillopathies. *Front Neural Circuits*, *15*, 701080. https://doi.org/10.3389/fncir.2021.701080

Winterdahl, M., Noer, O., Orlowski, D., Schacht, A. C., Jakobsen, S., Alstrup, A. K. O., Gjedde, A., & Landau, A. M. (2019). Sucrose intake lowers mu-opioid and dopamine D2/3 receptor availability in porcine brain. *Sci Rep*, *9*(1), 16918. https://doi.org/10.1038/s41598-019-53430-9

Yamaguchi, T., Danjo, T., Pastan, I., Hikida, T., & Nakanishi, S. (2013). Distinct roles of segregated transmission of the septo-habenular pathway in anxiety and fear. *Neuron*, *78*(3), 537–544. https://doi.org/10.1016/j.neuron.2013.02.035

Zaer, H., Fan, W., Orlowski, D., Glud, A. N., Jensen, M. B., Worm, E. S., Lukacova, S., Mikkelsen, T. W., Fitting, L. M., Jacobsen, L. M., Portmann, T., Hsieh, J. Y., Noel, C., Weidlich, G., Chung, W., Riley, P., Jenkins, C., Adler, J. R., Jr., Schneider, M. B.,...Stroh, A. (2022). Non-ablative doses of focal ionizing radiation alters function of central neural circuits. *Brain Stimul*, *15*(3), 586–597. https://doi.org/10.1016/j.brs.2022.04.001